

## Article

# Identification of Diagenetic Facies Logging of Tight Oil Reservoirs Based on Deep Learning—A Case Study in the Permian Lucaogou Formation of the Jimsar Sag, Junggar Basin

Ming Qi <sup>1</sup>, Changcheng Han <sup>1,2,\*</sup>, Cunfei Ma <sup>3,\*</sup>, Geng Liu <sup>1</sup>, Xudong He <sup>1</sup>, Guan Li <sup>1</sup>, Yi Yang <sup>1</sup>, Ruyuan Sun <sup>1</sup> and Xuhui Cheng <sup>1</sup>

<sup>1</sup> College of Geology and Mining Engineering, Xinjiang University, Urumqi 830017, China; 15029351462@163.com (M.Q.); 118791993946@163.com (G.L.); 17629057553@163.com (X.H.); m13596956922@163.com (G.L.); 13069628223@163.com (Y.Y.); sryyxt0910@163.com (R.S.); g17862106282@163.com (X.C.)

<sup>2</sup> Xinjiang Key Laboratory for Geodynamic Processes and Metallogenic Prognosis of the Central Asian Orogenic Belt, Xinjiang University, Urumqi 830047, China

<sup>3</sup> School of Geosciences, China University of Petroleum (East China), Qingdao 266580, China

\* Correspondence: hanchangcheng@xju.edu.cn (C.H.); mcf-625@163.com (C.M.)

**Abstract:** As a typical tight oil reservoir in a lake basin, the Permian Lucaogou Formation of the Jimsar Sag in the Junggar Basin has great potential for exploration and development. However, at present, there are few studies on the identification of the diagenetic facies of tight oil reservoir logging in the study area, and the control effect of diagenesis on tight oil reservoirs is not clear. The present work investigates the diagenesis and diagenetic facies logging of the study area, making full use of core data, thin sections, and logs, among other data, in order to understand the reservoir characteristics of the Permian Lucaogou Formation in the Jimsar Sag. The results show that the Lucaogou Formation has undergone diagenetic activity such as compaction, carbonate cementation, quartz cementation, and clay mineral infilling and dissolution. The diagenetic facies are classified according to mineral and diagenetic type, namely, tightly compacted facies, carbonate-cemented facies, clay mineral-filling facies, quartz-cemented facies, and dissolution facies. The GR, RT, AC, DEN, and CNL logging curves were selected, among others, and the convolutional neural network was introduced to construct a diagenetic facies logging recognition model. The diagenetic facies of a single well was divided and identified, and the predicted diagenetic facies types were compared with thin sections and SEM images of the corresponding depths. Prediction results had a high coincidence rate, which indicates that the model is of a certain significance to accurately identify the diagenetic facies of tight oil reservoirs. Assessing the physical properties of the studied reservoirs, dissolution facies are the dominant diagenetic facies in the study area and are also the preferred sequence for exploration—to find dominant reservoirs in the following stage.

**Keywords:** diagenetic facies; convolutional neural network; tight oil reservoir; Lucaogou Formation; Junggar Basin



**Citation:** Qi, M.; Han, C.; Ma, C.; Liu, G.; He, X.; Li, G.; Yang, Y.; Sun, R.; Cheng, X. Identification of Diagenetic Facies Logging of Tight Oil Reservoirs Based on Deep Learning—A Case Study in the Permian Lucaogou Formation of the Jimsar Sag, Junggar Basin. *Minerals* **2022**, *12*, 913. <https://doi.org/10.3390/min12070913>

Academic Editor: Ricardo Ferreira Louro Silva

Received: 19 June 2022

Accepted: 18 July 2022

Published: 20 July 2022

**Publisher's Note:** MDPI stays neutral with regard to jurisdictional claims in published maps and institutional affiliations.



**Copyright:** © 2022 by the authors. Licensee MDPI, Basel, Switzerland. This article is an open access article distributed under the terms and conditions of the Creative Commons Attribution (CC BY) license (<https://creativecommons.org/licenses/by/4.0/>).

## 1. Introduction

Tight oil refers to oil stored in reservoirs, such as tight sandstone and tight carbonate rock reservoirs, with a permeability of  $\leq 0.1 \times 10^{-3} \mu\text{m}^2$ , or oil with a nonheavy oil flow of  $\leq 0.1 \times 10^{-3} \mu\text{m}^2 \text{ (mPa}\cdot\text{s)}$  [1,2]. Tight oil reservoirs are currently one of the most important unconventional oil and gas resources in China's oil- and gas-bearing basins [3–5]. Compared to conventional reservoirs, tight oil reservoirs have the characteristics of low porosity and low permeability, and have great exploration and development potential [6–9]. In recent years, the production of tight oil reservoirs in China's Ordos and Junggar Basins has shown large-scale growth [10,11]. Tight oil reservoirs are buried at great depths, undergoing

a series of complex sedimentary and diagenetic processes during formation. Especially for tight oil reservoirs where source and storage coexist, their diagenesis is complex, and multiple diagenetic events can occur. Therefore, it is of great significance to know the influence of diagenesis on the quality of tight reservoirs.

As a typical tight oil reservoir in the Jimsar Sag of the Junggar Basin, the Permian Lucaogou Formation has seen significant breakthroughs in exploration and development in recent years [12]. Different scholars have carried out a large number of studies on reservoir characteristics, lithology types, sedimentary effects and sedimentary environments, source rock potential, and reservoir exploration and development potential in this area [13–17]. However, there are currently few studies on the identification of diagenetic facies in tight oil reservoir logging, and the control effect of diagenesis on tight oil reservoirs in the study area remains unclear.

For the accurate definition of diagenetic facies, different scholars have different formulations, but, in general, they all involve the diagenetic environment and diagenetic products under the action of the diagenetic environment; thus, diagenetic facies are widely used to evaluate reservoir quality [18–23]. Limited by the cost of cores, the study of diagenetic facies is relatively weak [24–26]. Considering the readability of logging data, an interpretation model for logging diagenetic facies can be established by comparing the diagenetic facies of the core well with the logging data to achieve accurate identification of the diagenetic facies in the intervals lacking core control [24].

The proposed method of identifying logging diagenetic facies has gradually expanded the prediction of diagenetic facies, from being in the intervals with core control to being in the intervals lacking core control [27]. There are several common methods for logging diagenetic facies: (1) Rendezvous diagram method: identification standards for different diagenetic facies are established according to typical logging curves. The accuracy of diagenetic identification is affected by the limitation of selecting the number of logging curves [27,28]. (2) Spider diagram method: the logging response characteristics of different diagenetic facies are projected onto the axis to achieve facies identification; the advantage of this method is that it is relatively simple to apply [29]. (3) Diagenetic facies strength calculation method: the quantitative characterization of diagenetic facies by calculation of diagenetic strength parameters (compaction porosity loss, cementation porosity loss, etc.) [30–32]. (4) Mathematical method: the identification of typical diagenetic facies by summarizing the logging response characteristics of different types of diagenetic facies, including principal component analysis, Fisher's discriminant, neural network prediction, etc. [18,33]. Compared with traditional linear prediction, Hinton first proposed deep learning in 2006 to solve the problem of the local optimal solution in traditional neural networks [34]. At present, deep learning includes a variety of evolutionary methods, such as convolutional neural networks (CNNs), recurrent neural networks (RNNs), deep belief neural networks (DBNs), etc. CNNs have been widely used in image processing, speech recognition, and other fields [35,36]; CNNs are also widely used in earth science, including lithology identification, seismic data processing, and reservoir quality evaluation, but it is seldom used in logging diagenetic facies [37–39].

The purpose of this paper is to identify and predict the diagenetic facies in the intervals lacking core control by a convolution neural network. Taking the Permian Lucaogou Formation in the Jimsar Sag as the research object, the diagenetic facies types in the study area are divided according to mineral and diagenetic types. Based on the relationship between diagenetic facies and logging curves, a prediction model is established by introducing the convolutional neural network (CNN) to accurately predict the diagenetic facies in intervals lacking well core control.

### 2. Regional Geological Setting

The Jimsar Sag is located in the eastern Junggar Basin, in a tectonic setting which corresponds to the sub-primary depression of the eastern uplift of the Junggar Basin [13]. It is bounded by the Jimsar Fault to the north and the Santai Fault in the south, with a total area of about 1500 km<sup>2</sup> [40] (Figure 1). The Jimsar Sag underwent multistage tectonic movements during its formation, mainly during the Hercynian, Indochina, and Yanshan periods [13], with the bottom-up development of Carboniferous, Permian, Triassic, and Jurassic strata [41,42] (Figure 2). The Permian Lucaogou Formation is the main unit for tight oil exploration and development in the Jimsar area. It occurs across the entire depression, with a thickness that generally varies from 200 to 350 m [43]. The rock types that comprise the Lucaogou Formation are complex, including dolomitic siltstone, mudstone, and dolomite as the dominant lithologic units, with generally fine grain sizes. This makes it a typical tight oil reservoir, with good prospects for exploration and development.

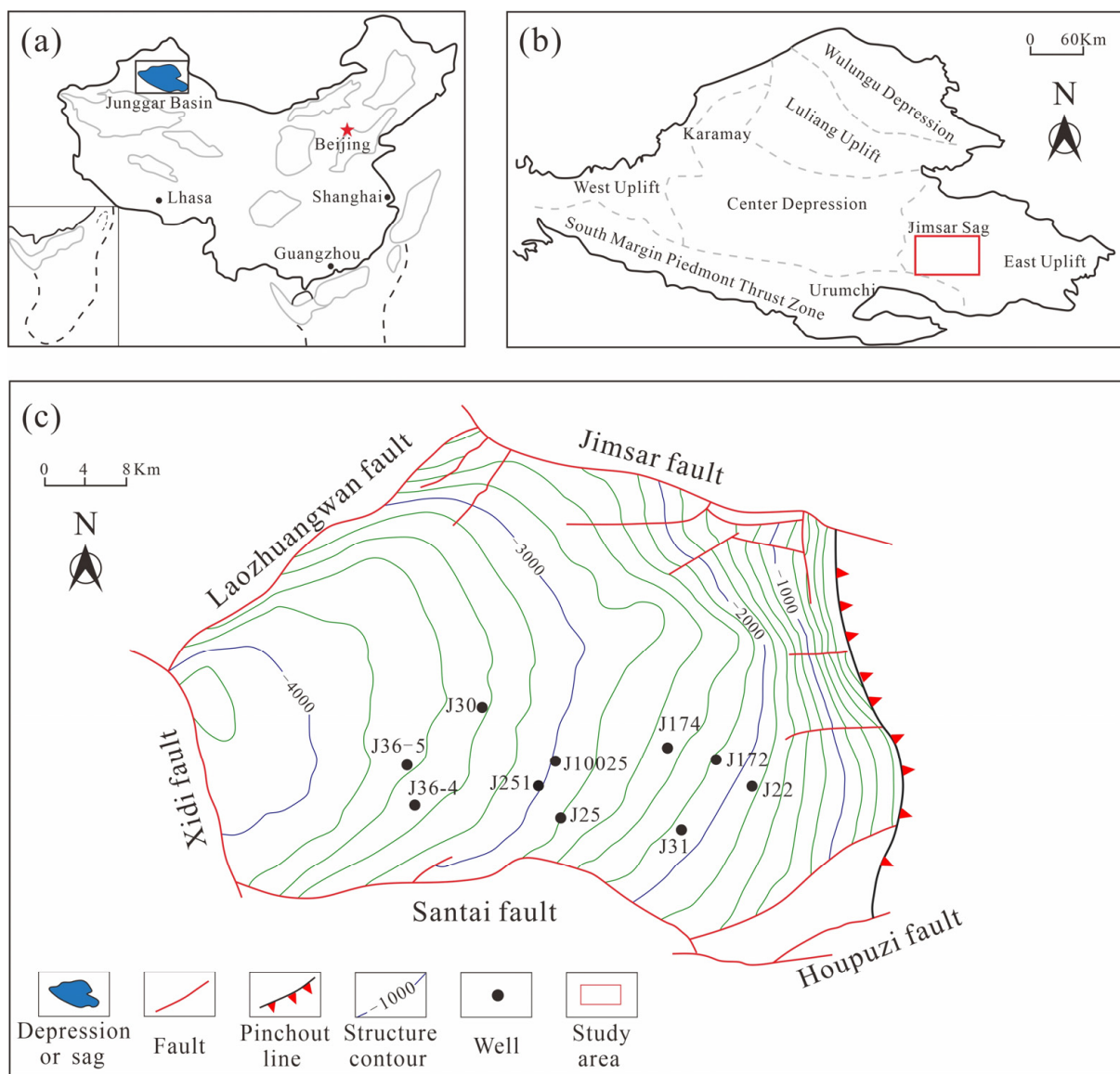


**Figure 1.** (a) Location map of the Junggar Basin in China, (b) location map of the Jimsar Sag in the Junggar Basin, and (c) regional structural map of Lucaogou Formation in the Jimsar Sag [40,41].

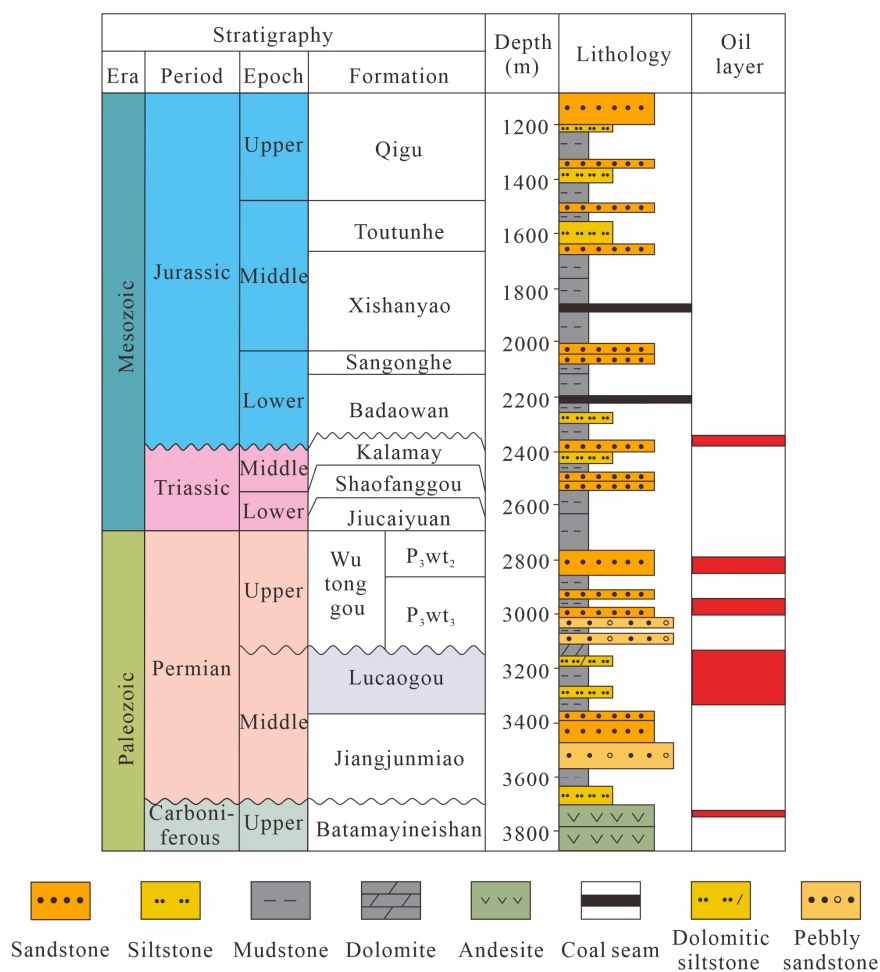


Figure 2. Development characteristics of the Lucaogou Formation and its upper and lower strata in the Jimsar Sag [42].

### 3. Materials and Methods

#### 3.1. Core Test and Geophysical Logging Database

The identification of diagenesis and diagenetic facies logging mainly uses logging data and core analysis data. There are 53 logging wells and 22 core wells in the study area. A total of 174 samples from the core well were used for routine physical property analysis, and the samples selected for measuring porosity and permeability were core cylinders with a diameter of 2.5 cm and a length of 5 cm. The cylinders were drilled along the horizontal method of the core, and the physical properties of the reservoir such as porosity and permeability were measured. The resistivity log (RT), gamma ray log (GR), acoustic log (AC), compensated neutron log (CNL), and density log (DEN) from the well logging data were selected to demonstrate diagenetic facies.

##### 3.1.1. XRD

XRD was used to quantitatively determine the relative mineral content of 27 representative rock samples from the study area. A RINT-TTR3 X-ray diffraction instrument (RINT-TTR3, Rigaku Corporation, Tokyo, Japan) was used for X-ray diffraction whole-rock analysis, with a scanning speed of 0.25°/min and a scanning range of 2.5°~60°. The rock samples were ground to 200 mesh, the mineral powder was separated from the clay powder and dried, and the mineral type and content were determined according to the characteristic peak intensity of different minerals in the diffractogram.

### 3.1.2. Thin Sections

Two kinds of thin sections were prepared for optical microscopy: fluorescent thin sections of 36 samples and casting thin sections of 317 samples. The fluorescent thin sections had a thickness of 0.05 mm without coverslips, and were studied using a Zeiss Axio Image Z1 microscope (Axio Image Z1, Zeiss, Oberkochen, Germany), which can mainly distinguish pores from mineral types by their fluorescent color. The thickness of the casting thin section was 0.03 mm; the sample holder was filled with blue epoxy resin before microscopic observation, dyed with alizarin red and ferricyanide, and the pores and carbonate cement in the rock (including calcite and dolomite cement) were clearly observed after dyeing. The same microscope mentioned above was used to observe pore types and carbonate minerals.

### 3.1.3. SEM

The scanning electron microscope (SEM) (FIB-SEM, Zeiss, Oberkochen, Germany) was used to make observations of rock pore structure, mineral types, and diagenesis at the micro-nanometer scale. A Zeiss SEM was used with a minimum resolution of 1.2 nm and a magnification of 25 to 2000  $\times$ . A total of 312 samples were analyzed by SEM. Samples were pretreated before microscopic observation, polished with an argon ion beam, and their surfaces were sprayed with Au to improve conductivity for optimal microscopic observation.

### 3.1.4. Logging Curve Preprocessing

Different logging series cause errors during the establishment of the model due to different dimensions. Therefore, the sample dataset and test dataset need to be normalized before establishing different diagenetic facies log response databases to eliminate the influence of dimensions between different logging series. Normalization of the selected conversion function, such as Equation (1), can be mapped to [0~1]. The processed sample dataset and the test dataset have independence, improving the accuracy of the model.

$$X_i = \frac{x_i - x_{min}}{x_{max} - x_{min}} \quad (1)$$

$X_i$  is normalized data;  $x_i$  is the actual logging data;  $x_{min}$  is the minimum value of the actual logging curve data;  $x_{max}$  is the maximum value of the actual logging curve data.

## 3.2. Convolutional Neural Network (CNN)

CNN is a deep feedforward neural network. Compared with the traditional neural network model, the increase in feature extractors in the combination of the convolutional layer and pooling layer effectively reduces the parameters of the neural network, and solves the problem of having too many model parameters and too much training time when the number of hidden layers is too large [39]. The basic structure of a convolutional neural network includes the input layer, the convolutional layer, the pooling layer, the fully connected layer, and the output layer (Figure 3). Commonly, a 1D-CNN is used in the fields of sequence modeling and natural language processing; a 2D-CNN is commonly used in the fields of computer vision and image processing; and a 3D-CNN adds a temporal dimension, which can extract temporal and spatial features at the same time, and is often used in CT imaging, behavior recognition, video processing, etc. [44]. The problem studied in this paper belongs to the sequence model; therefore, the 1D-CNN method was used (Figure 3). In the most common convolutional neural networks, the convolutional layer and pooling layer alternately set up connections. Each neuron in each feature plane in the convolutional layer is locally connected to the input data of the previous layer, and the input data is folded with the convolutional kernel plus the bias value; thus, such a neural network is named a convolutional neural network.

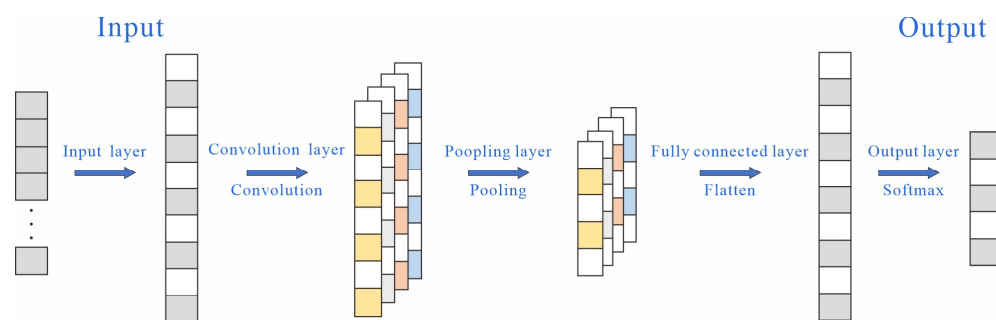


**Figure 3.** Structure diagram of 1D-CNN.

(1) Convolutional layer: The convolutional layer is the most important part of the convolutional neural network, which extracts the eigenvalues of the input data by computing them with the convolutional kernel. The selection of the convolutional nuclei has an important impact on feature extraction [45].

(2) Pooling layer: The pooling layer mainly reduces the amount of computation in the training process by reducing the dimension of the input data, and further extracts the feature vectors [46]. Common methods include maximum pooling, mean pooling, and random pooling.

(3) Fully connected layer: The fully connected layer is generally located at the end of the convolutional neural network, and the output information of the convolution layer or the pool layer is sorted out [35].

This 1D-CNN consisted of an input layer, six convolution layers with the hyperbolic tangent function  $\tanh$  (hyperbolic tangent function) as the activation function, a pool layer added after every two convolution layers to retain the main features, a full connection layer with softmax as the activation function, and an output layer. The loss function used the cross-entropy loss function, and the optimizer was the Adam function. Tensorflow was installed in the Anaconda software, Keras was used as the network building tool, and the Python programming language was used for 1D-CNN model building.

### 3.3. Use of Method Flows during Model Building

Based on logging and geological data of the study area, the main characteristics of the reservoir of the Permian Lucaogou Formation of the Jimsar Sag were studied, including rock types, physical properties, and pore types, among other characteristics. Thus, the dominant diagenetic type in the formation of tight oil reservoirs in the study area was clarified. Based on the definition of diagenetic facies, combined with the core analysis data of the thin section, the diagenetic facies type of the core well section was determined, and the diagenetic facies type was combined with the typical logging curve to establish a diagenetic facies logging database. The selected diagenetic facies type and logging curve were used as training samples and model detection samples the CNN, and a diagenetic facies prediction model of intervals lacking core well control was established.

## 4. Results

### 4.1. Basic Characteristics of the Reservoir

#### 4.1.1. Petrological Features

The lithologies of the tight oil reservoirs of the Lucaogou Formation are diverse (Figure 1b), and the composition of minerals is complex (Table 1). The content of clay minerals in the Lucaogou Formation is low (12.5%), and the main components are smectite, illite, kaolinite, chlorite, and I/S. The illite and smectite contents are higher, accounting for 39.8% and 22.23%, respectively. The contents of the I/S mixed-layer and chlorite are slightly lower, accounting for 17.46% and 16.8%, respectively, and the least abundant of the clay minerals is kaolinite, accounting for 10.5% of the clay mineral infill (Figure 4). The Lucaogou Formation has undergone diagenetic activity such as compaction, carbonate

cementation, quartz cementation, and clay mineral infilling and dissolution. Quartz, clays (illite and authigenic chlorite), and carbonates are the major pore-filling constituents.

**Table 1.** XRD analysis of reservoir rocks in the Lucaogou Formation of Jimsar Sag.

Name	Depth/m	Mineral Composition (%)							
		Clay	Dolomite	Calcite	Pyrite	Potassium Feldspar	Quartz	Anorthite	Ankerite
J174	3217.98	20.0	15.2	14.0	—	3.0	17.7	30.1	—
J174	3259.65	7.5	44.5	0.3	—	4.0	22.5	21.2	—
J174	3283.38	12.4	17.7	7.4	—	4.9	17.5	40.1	—
J174	3285.57	11.8	31.3	—	0.5	5.8	18.3	32.3	—
J174	3295.85	17.0	23.5	2.2	0.6	6.5	20.6	29.6	—
J174	3335.41	10.8	8.0	41.1	11.0	1.3	10.1	9.8	—
J251	3614.10	8.7	28.9	11.4	2.4	3.7	28.1	16.8	—
J251	3632.13	7.7	11.7	33.0	3.4	14.4	18.8	11.0	—
J251	3773.12	13.2	25.4	12.2	—	1.7	25.6	21.9	—
J36-5	4348.70	33.1	—	2.2	0.8	—	61.2	2.7	—
J36-5	4349.84	46.4	—	0.5	0.5	—	49.8	2.8	—
J36-5	4353.98	45.5	—	1.6	0.9	—	46.9	4.2	0.9
J36-4	4340.35	4.9	—	1.8	0.2	—	30.0	33.0	30.1
J36-4	4344.70	5.5	—	0.4	0.4	6.0	26.3	30.4	31.0
J36-4	4345.36	0.9	—	81.1	0.6	—	6.9	8.9	1.5
J36-4	4346.47	28.5	—	34.9	—	1.5	14.4	11.3	9.5
J36-4	4347.74	5.5	—	—	0.2	6.7	26.0	36.1	25.5
J36-4	4353.11	5.1	—	29.0	—	2.4	20.0	17.6	25.9
J36-4	4356.47	6.6	—	10.3	0.3	8.3	36.0	38.5	—
J36-4	4358.24	1.3	—	44.2	—	0.9	37.7	7.6	8.3
J36-4	4359.12	5.1	—	17.3	0.3	—	14.1	40.2	23.0
J36-4	4362.32	7.6	—	7.3	13.8	—	28.0	33.4	10.0
J36-4	4363.71	3.1	—	13.6	0.2	4.0	11.7	47.8	19.6
J36-4	4368.11	6.2	—	37.1	0.5	1.7	37.5	15.7	1.4
J36-4	4369.50	8.1	—	32.8	0.3	—	25.5	28.0	5.3
J36-4	4374.79	9.0	—	9.3	4.9	—	21.3	44.0	11.5
J36-4	4380.46	5.8	—	33.6	0.6	—	26.1	21.3	12.7
Average		12.5	22.9	19.1	2.1	4.5	24.7	23.5	14.4

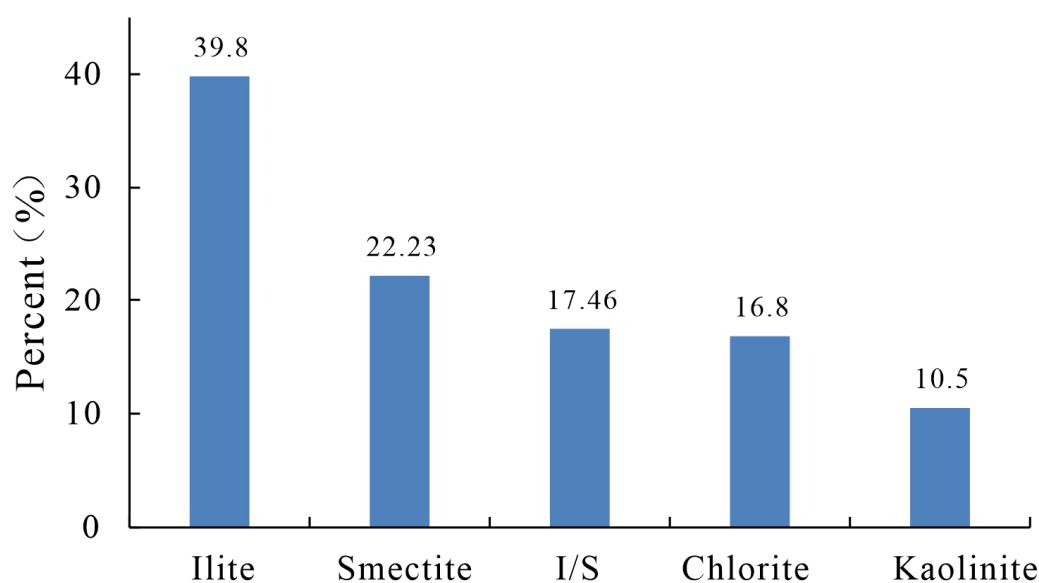


**Figure 4.** Clay mineral analysis results of the Permian Lucaogou Formation in the Jimsar Sag.

The grain size of the rock is fine, and various sedimentary structures such as wavy bedding and stylolite are developed (Figure 5a–c). The lithology of the reservoir is divided into mixed fine-grained rocks, clastic rocks, and carbonate rocks (Figure 5d–i). The mixed fine-grained rocks are mainly composed of clastic rocks (35.2%–47.5%) and carbonate rocks (52.5%–64.8%), and they are characterized by lamellar and massive interactions (Figure 5d,e). The clastic rocks mainly include dolomitic siltstone, argillaceous siltstone, fine calcareous sandstone, and fine argillaceous sandstone. Quartz clastic bands and clay veins are mutually visible in dolomite siltstone (Figure 5f). Fine calcite grains are distributed across a large area with irregular edges in fine calcareous sandstone (Figure 5g). Carbonate rocks mainly include limestone, argillaceous dolomite, and argillaceous limestone. The grain size of rocks is generally fine, with fine carbonate sandstones and siltstones as the main lithologies (Figure 5h,i).

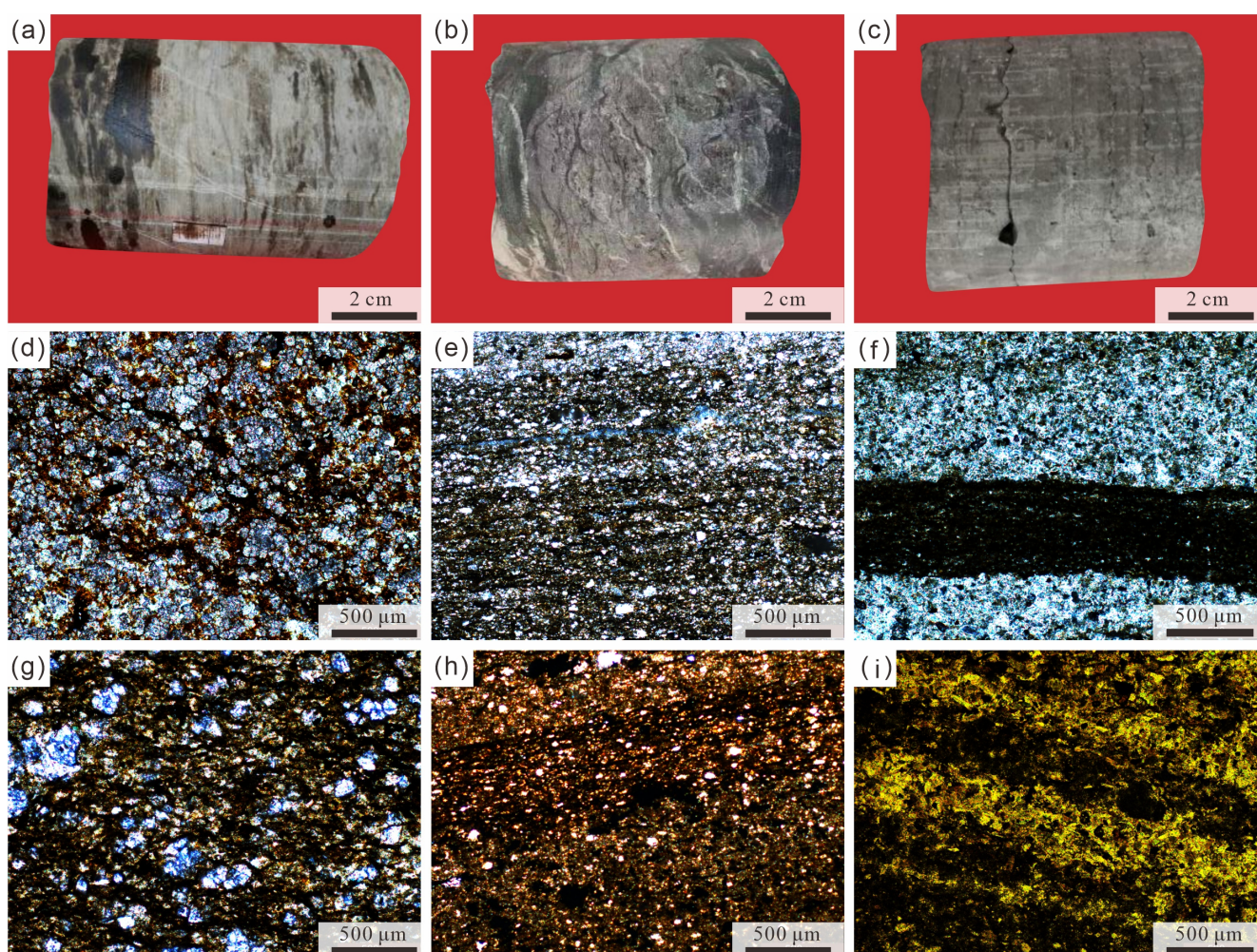


**Figure 5.** Reservoir rock types of the Permian Lucaogou Formation in the Jimsar Sag. (a) Gray calcareous siltstone, developmental wavy bedding, J36-4, 4346.13 m; (b) gray sandstone, filled calcite strip, developmental wave layering, kneading structure, J10025, 3567.5 m; (c) green argillaceous siltstone, developmental stylolite, J10025, 3618.1 m; (d) lamellar and blocky interaction of mixed fine-grained rock, J36-4, 4373.46 m, PPL; (e) lamellar mixed fine-grained rock, J36-4, 4376.48 m, PPL; (f) lamellar dolomitic siltstone, J36-4, 4340 m, PPL; (g) block-like, fine, calcareous sandstone, J36-4, 4369.5 m, PPL; (h) block limestone, J36-4, 4345.36 m, PPL; (i) lamellar argillaceous dolomite, J36-4, 4353.33 m. PPL: plane-polarized light.

#### 4.1.2. Reservoir Physical Property Characteristics

The results of a conventional physical property analysis show that the porosity of the tight oil reservoirs was 2.42%–18.2%, with an average of 8.92%, and had a permeability of 0.004 mD–0.75 mD, with an average of 0.064 mD. This shows that the overall physical properties of the reservoir were poor, reservoir densification was high, and the correlation between reservoir porosity and permeability was good (Figure 6).

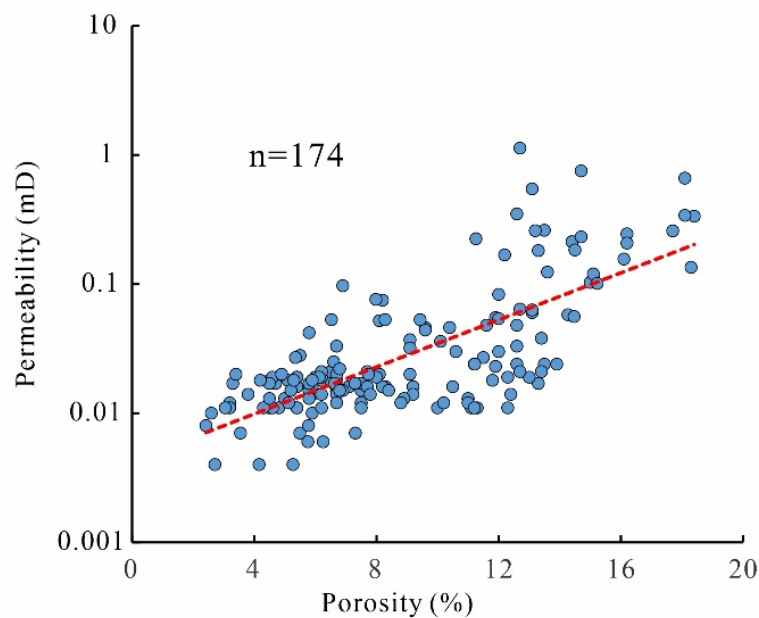


**Figure 6.** Relationship between porosity and permeability of the Permian Lucaogou Formation.

#### 4.1.3. The Types of Storage Space

Both primary and secondary pores exist in the reservoir space of the study area (Figure 7a–i). Secondary pores mainly include secondary dissolution pores, intergranular pores, microcracks, etc. Primary pores include primary intergranular pores and residual intergranular pores.

##### (1) Secondary dissolution pores

Secondary dissolution pores were the main reservoir spatial types developed in the Lucaogou Formation and were present in different lithologies (Figure 7a,b). The degree of development of secondary dissolution pores is mainly related to the dissolution of unstable components such as feldspar, tuff components, and rock fragments [47]. Potassium feldspar, albite feldspar, and other feldspars and their alteration products are strongly eroded by acid circulation, forming secondary dissolution pores.

##### (2) Intergranular pores

Various types of intergranular pores were developed in the Lucaogou Formation, mainly between clay minerals, feldspar, quartz, calcite, and dolomite (Figure 7c–e). Dolomite and calcite intergranular pores were the most common types of intergranular pores in the study area.

##### (3) Microcracks

Microcracks are structural fractures that cut through mineral grains in the rock, commonly through high-angle microcracks, with jagged morphologies. Nonstructural cracks mainly communicate intergranular pores, which are often filled with asphaltene. The study area mainly developed diagenetic micro-fractures filled with carbonate minerals and had fewer structural cracks (Figure 7f,g).

## (4) Primary pores

Primary pores mainly refer to residual intergranular pores remaining after a series of diagenetic processes (compaction, cementation, dissolution) experienced by the reservoir during formation [39]. The thin sections and SEM images mainly showed primary pores that were not filled with heterogeneous materials or cement, organic matter, and the remaining intergranular pores after being filled with clays and authigenic minerals. Pore boundaries were clear and often unevenly distributed (Figure 7h,i).

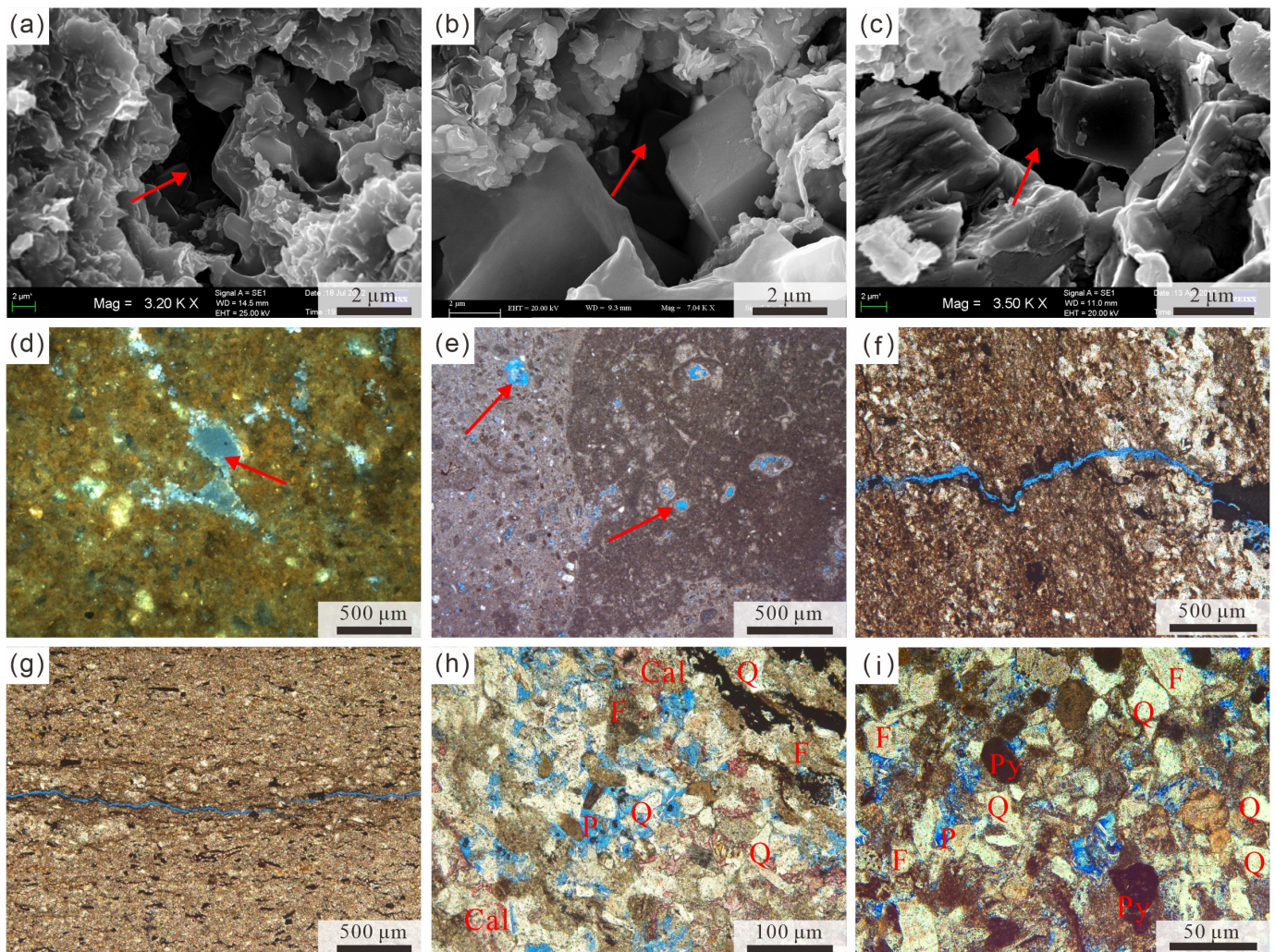


**Figure 7.** Reservoir space types of the Permian Lucaogou Formation in the Jimsar Sag. (a) Gray argillaceous siltstone, development of dissolution pores in the matrix, J174, 3334.68 m, SEM; (b) gray, argillaceous, silty sandstone, dissolution of potassium feldspar grains and dissolution pores in the matrix, J174, 3333.76 m, SEM; (c) gray marl rock, intragranular dissolution pores and intergranular pores, J174, 3182.43 m, SEM; (d) gray calcareous siltstone, dolomite intercrystalline pores, J174 3144.84 m, fluorescence thin section; (e) gray marl, calcite intercrystalline pores, J174, 3112.09 m, PPL; (f) gray dolomitic siltstone, developmental microcracks, J251, 3777.44 m, PPL; (g) gray marl, developmental microcracks, J31, 2712.85 m, PPL; (h) gray, fine, calcareous sandstone, residual intergranular pores containing calcite cement, J31, 2725.16 m, PPL; (i) gray calcareous siltstone, residual intergranular pores containing pyrite, J174, 3142.13 m, PPL. Cal: calcite; Q: quartz; F: feldspar; Py: pyrite; P: pores; PPL: plane-polarized light. Red arrows indicate dissolution pores, intergranular pores.

#### 4.2. Diagenetic Facies Classification

The theoretical basis of diagenetic facies research is diagenesis, and the main basis for the classification and naming of diagenetic facies is the study of diagenetic minerals [48]. Classifying diagenetic facies requires determining the type and intensity of diagenesis experienced by the sediment, on the basis of which special minerals are indicative in the diagenetic process. These are observed by studying the thin section of the core well. In this paper, diagenetic facies are divided and named according to the principle of mineral type and diagenetic type. Compaction is the main factor controlling reservoir quality. However, due to the influence of other factors, the intensity of compaction in space is uneven. The ZTR index of heavy minerals ranges from 0.2 to 10.1, with an average of 2.8. This shows that the Lucaogou Formation has low composition maturity, low reservoir resistance to compaction, and a greater influence on compaction. Therefore, the rocks in areas where compaction is relatively strong are relatively dense and have poor physical properties—these are classified as tightly compacted facies. Dissolution can effectively improve total porosity, and dissolved components are mainly unstable minerals such as feldspar, rock fragments, and tuff components—the areas dominated by dissolution are classified as dissolution facies. Quartz overgrowths fill pores, and reduce porosity and reservoir quality—facies with this feature are classified as quartz-cemented diagenetic facies. Carbonate cementation is widely developed in the study area, found in mainly calcite, iron calcite and ankerite, with the mass fraction of 1%~32% and with an average of 7.22%. Carbonate cement and clay cement influence porosity to a different degree. For instance, clay cement mainly appears in the form of pore filling. The two main diagenetic control areas are each classified as diagenetic facies, and are named carbonate-cemented facies and clay mineral-filling facies, respectively. Thus, the Lucaogou Formation can be divided into five types of diagenetic facies: tightly compacted facies, carbonate-cemented facies, clay mineral-filling facies, quartz-cemented facies, and dissolution facies. Logging curves that are sensitive to diagenetic facies-type indications mainly include the gamma ray log (GR), resistivity log (RT), acoustic log (AC), density log (DEN), and compensated neutron log (CNL) [18,49]. Therefore, when establishing the diagenetic facies logging database, the differences between the five logging curves of different diagenetic facies types were considered. Characteristics of the well log response for identifying five diagenetic facies were summarized, and the well log parameters of different diagenetic facies were provided (Table 2, Figure 8).

**Table 2.** Characteristics of different diagenetic logging responses.

Diagenetic Facies	GR/API	AC/ $\mu\text{s}\cdot\text{ft}^{-1}$	DEN/ $\text{g}\cdot\text{cm}^{-3}$	RT/ $\Omega\cdot\text{m}$	CNL/%
Tightly compacted facies	67.5~138.8 (101.2)	66.7~78.4 (72.4)	2.3~2.6 (2.5)	6.1~40.3 (14.8)	18.6~30.3 (23.7)
Carbonate-cemented facies	58.5~97.5 (75.7)	72.5~94.6 (78.6)	2.0~2.5 (2.4)	10.9~74.0 (36.3)	18.5~35 (22.9)
Quartz-cemented facies	61.6~112.5 (88.3)	67.4~87.5 (74.6)	2.17~2.5 (2.4)	14.4~83.8 (31.5)	18.9~36.4 (25.2)
Clay mineral-filling facies	73.8~111.9 (89.7)	76.6~94.6 (84.6)	2.2~2.5 (2.36)	10.7~73.9 (41.2)	26~41.9 (32)
Dissolution facies	38.0~87.9 (65.6)	70.1~93.8 (80)	2.1~2.6 (2.3)	112.7~273.1 (177.9)	22.7~40.8 (30.4)

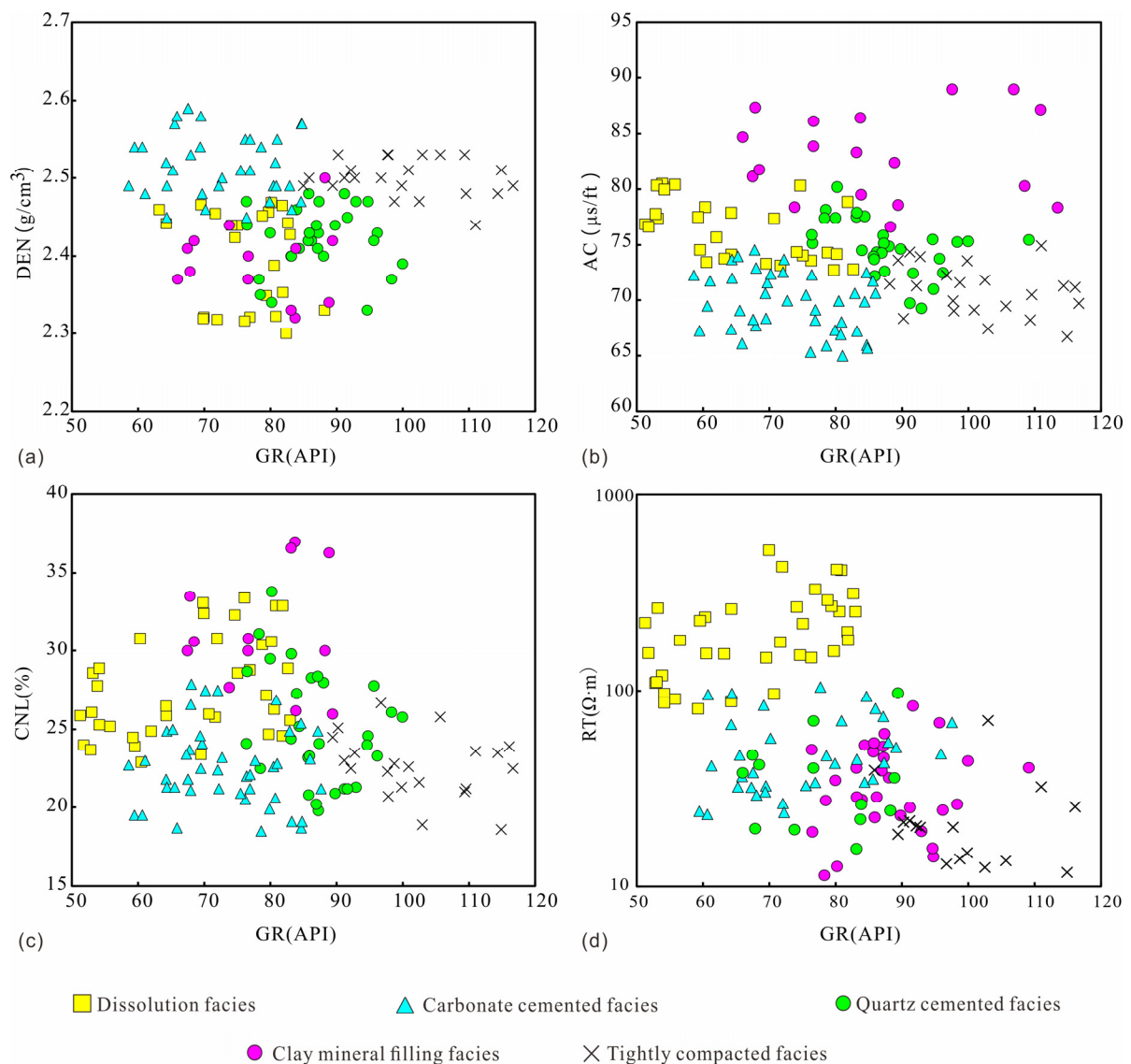


**Figure 8.** Different diagenetic facies and their well log values. Plots of gamma ray log (GR) versus (a) density log (DEN), (b) acoustic log (AC), (c) compensated neutron log (CNL) and (d) resistivity log (RT) values.

## 5. Discussion

### 5.1. Different Diagenetic Facies Types and Their Logging Response Characteristics

The study of different diagenetic facies mainly relies on core observation and thin section identification results to determine whether the difference in the petrological and mineralogical characteristics of the diagenetic facies led to a difference in the response characteristics of the logging curve [50]. The core-to-log depth matching was performed by correlating the density logging (DEN) signature with the core experiment, and a diagenetic facies recognition model was established by analyzing the logging response characteristics of different diagenetic facies to achieve accurate identification of diagenetic facies using logging data.

### 5.1.1. Dissolution Facies

Dissolution is a constructive diagenetic effect, which mainly dissolves various types of feldspars, rock fragments, and volcanic tuff components in skeletal grains (Figure 9a,b), which can significantly increase the pore space of the reservoir and improve reservoir quality. The feldspar content in Lucaogou is high, which is conducive to the formation of dissolution pores. The development of dissolution pores made the DEN values of these diagenetic facies low (average  $2.3 \text{ g/cm}^3$ ). AC values were high ( $>70 \text{ } \mu\text{s/ft}$ ), and CNL values ranged from 22.7% to 40.8%; dissolution facies had lower GR values (38.0 API~87.9 API) and higher RT values ( $>112 \text{ } \Omega\cdot\text{m}$ ) due to their high oil potential (Table 2, Figures 8 and 10).

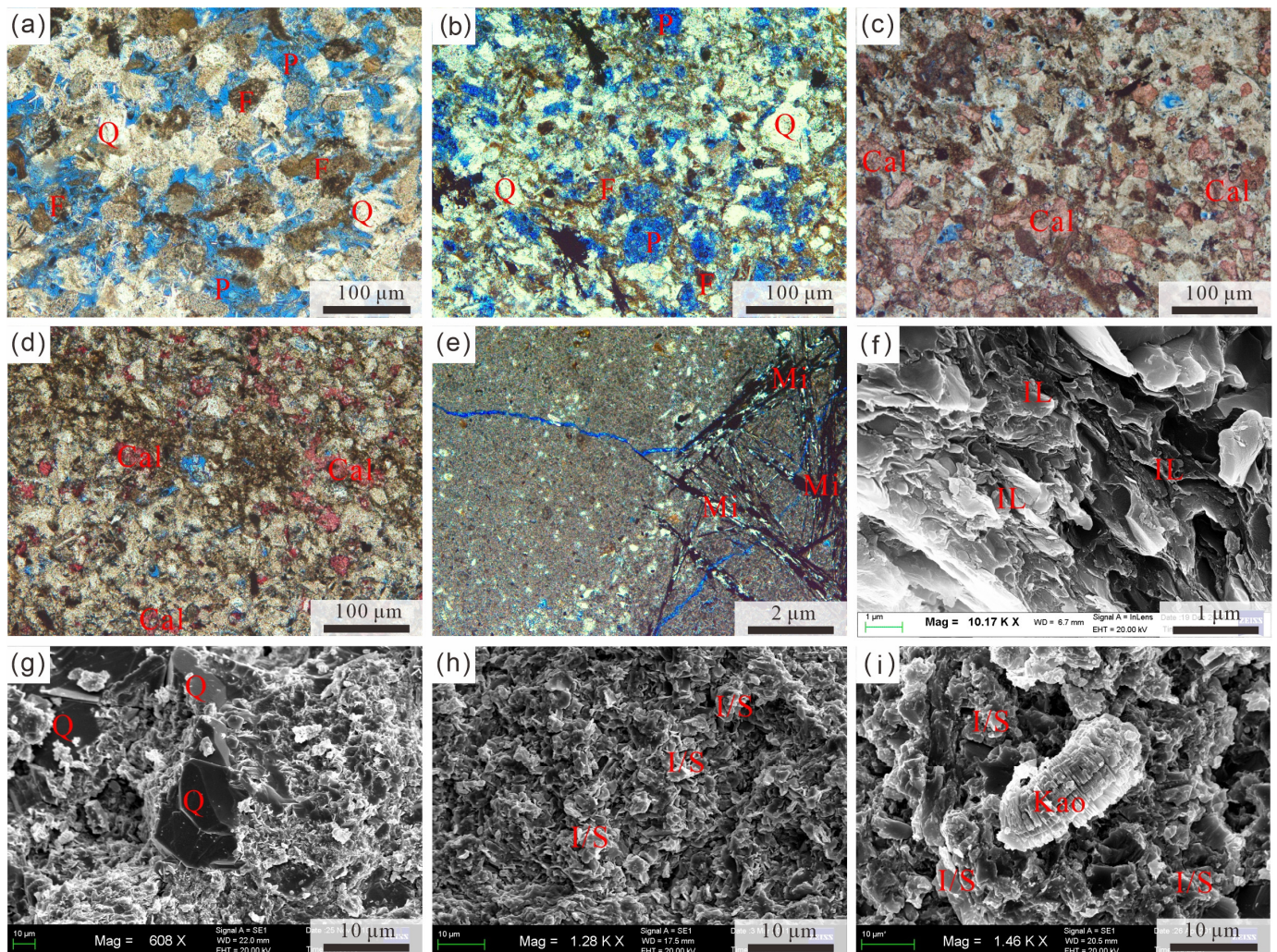


**Figure 9.** Different types of diagenesis in the Permian Lucaogou Formation of the Jimsar Sag. (a) Dissolution of fine, gray, calcareous sandstone and dissolution of feldspar grains, J31, 2725.36 m, PPL; (b) dissolution of tuff sludge, a tuff component dissolution phenomenon, J174, 3269.74 m, PPL; (c) calcite-cemented gray mudstone, J174, 3199.99 m, PPL; (d) gray carbonate-cemented siltstone, calcite cement, J251, 3759.40 m, PPL; (e) compacted, gray, calcareous siltstone. Plastic deformation of mica affected by compaction, J174, 3268.48 m, PPL; (f) compacted, dark gray, argillaceous dolomite. Directional arrangement of illite, J30, 4144.86 m, SEM; (g) fine, siliceous-cemented siltstone (argillaceous), quartz overgrowths, J172, 2927.9 m, SEM; (h) clay mineral cementation, dark gray dolomite mudstone, I/S distributed in the matrix, J22, 2553.92 m, SEM; (i) clay mineral cementation, silty-sandy mudstone, vermiform kaolinite, J25, 3412.54 m, SEM. Mi: mica; Cal: calcite cementation; I/S: mixed-layer illite/smectite; Kao: kaolinite; Q: quartz; F: feldspar; IL: illite; P: pores; PPL: plane-polarized light.

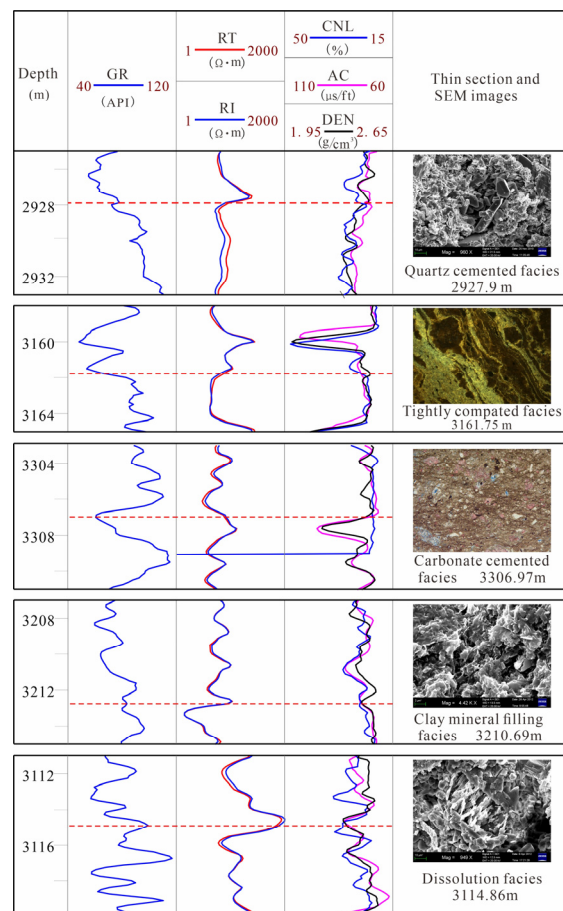


**Figure 10.** Characteristics of different diagenetic facies logging curves and corresponding thin sections and SEM images.

### 5.1.2. Carbonate-Cemented Facies

The identification results of the rock slices of 36 samples in the study area showed that carbonate cementation is widely developed in the study area, mainly through calcite, iron calcite, and iron dolomite, with a mass fraction from 1% to 32% and with an average of 7.22%. Carbonate cements, such as calcite and dolomite, developed in dissolved reservoir pores while blocking pore space and reducing reservoir quality [51,52]. Therefore, the carbonate cement facies is destructive, and the cement produced by multistage carbonate cementation fills the tectonic cracks, increasing the damage to the physical properties of the reservoir (Figure 9c,d). The presence of carbonate cement resulted in the diagenetic facies having medium-high RT values (average 36.3 Ω·m), high DEN values (average 2.4 g/cm<sup>3</sup>), and lower AC values (average 78.6 μs/ft), in addition to lower CNL values (average 22.9%) (Table 2, Figures 8 and 10).

### 5.1.3. Tightly Compacted Facies

Compaction occurs throughout the entire diagenetic process and is considered to be destructive diagenesis. Mechanical compaction in the Lucaogou Formation is common, and the pressure solution is less developed. The ZTR index of heavy minerals shows that the Lucaogou Formation has a greater influence on compaction, resulting in the destruction of a large number of primary pores and poor reservoir properties [51,52]. The content of plastic grains in siltstone is high, and it has evident characteristics of strong compaction effects such as plastic particle deformation, particle line contact, and mineral orientation arrangement (Figure 9e,f). In the tightly compacted facies, the presence of clay minerals, soft rock, and micas led to the highest GR values (average 101.2 API), high DEN values

(average  $2.5 \text{ g/cm}^3$ ), lower AC values ( $72.4 \text{ } \mu\text{s/ft}$ ), high CNL values (average 23.7%), and low RT values (average  $14.8 \text{ } \Omega\cdot\text{m}$ ) as important indicators for identifying compacted facies (Table 2, Figures 8 and 10).

#### 5.1.4. Quartz-Cemented Facies

Siliceous cement is generally developed in reservoirs of the Lucaogou Formation, mainly in the form of quartz overgrowths (Figure 9g). Feldspar grains produce a large amount of  $\text{SiO}_2$  during the dissolution process, thus providing an adequate source of material for quartz overgrowths; therefore, this process is often accompanied by the dissolution of feldspar grains. Because of the low solubility of  $\text{SiO}_2$  in the closed system composed of sand and mudstone, there is basically no external ion source in the siliceous cement of the Lucaogou Formation. Therefore, the endogenous source becomes the only material source of siliceous cement, mainly through the transformation of clay minerals and the dissolution of feldspar grains. The higher the quartz content in the mineral composition, the more obvious the phenomenon of siliceous cementation is, and the more common the phenomenon of quartz overgrowths becomes [52,53]. Compared with the relatively high GR values of the tightly compacted facies, the GR values of the quartz-cemented facies were lower (average 88.3 API), DEN values were medium and high (average  $2.4 \text{ g/cm}^3$ ); and AC values were lower (average  $74.6 \text{ } \mu\text{s/ft}$ ) (Table 2, Figures 8 and 10).

#### 5.1.5. Clay Mineral-Filling Facies

Clay mineral cements mainly include honeycomb I/S cement, filamentary illite, flaky cement, fluffy ball authigenic chlorite, and other minerals (Figure 9h,i). The Lucaogou Formation mainly developed with two-stage clay mineral cementation, where the primary pores and the flaky chlorite in the dissolution pores reduced the connectivity of the pore roar, and the presence of the I/S mixed-layer filled the pores [52,54,55]. Compared with the tightly compacted facies, the clay mineral-filling facies had lower mineral content and, therefore, moderate GR values (average 85.4 API). The presence of clay minerals made DEN values relatively low (average  $2.36 \text{ g/cm}^3$ ), AC values were high (average  $84.6 \text{ } \mu\text{s/ft}$ ), and there were high CNL values (average 32%) (Table 2, Figures 8 and 10).

### 5.2. Impact of Diagenetic Facies on Reservoir Quality of Tight Oil

Different diagenetic facies combinations lead to different porosity characteristics and physical properties of reservoirs. The differences in different diagenetic facies types are mainly reflected in the composition of diagenetic minerals; thus, the influence of different diagenetic facies types on reservoir quality can be determined by analyzing the main diagenetic minerals.

Carbonate cementation in the study area was generally developed as calcite, but also included iron calcite and (iron) dolomite. The relationship between pore content and cement content established by Houseknecht can indicate the effect of compaction and cementation on reservoir porosity reduction, and clearly reveals the primary and secondary causes of reservoir densification [56]. Carbonate cement content has a clear negative correlation with porosity; therefore, carbonate cementation can be considered to be the main factor in the decrease in porosity of tight oil reservoirs in the Lucaogou Formation (Figure 11a). Carbonate cements can fill the primary intergranular pores and, therefore, reduce the porosity of reservoirs [30]; when the carbonate cement completely fills the pore space, the quality of the reservoir becomes so poor that it may become the seepage barrier of fluid flow. Carbonate cement causes obvious pore loss in the carbonate cement phase, which becomes an obvious destructive diagenetic facies.

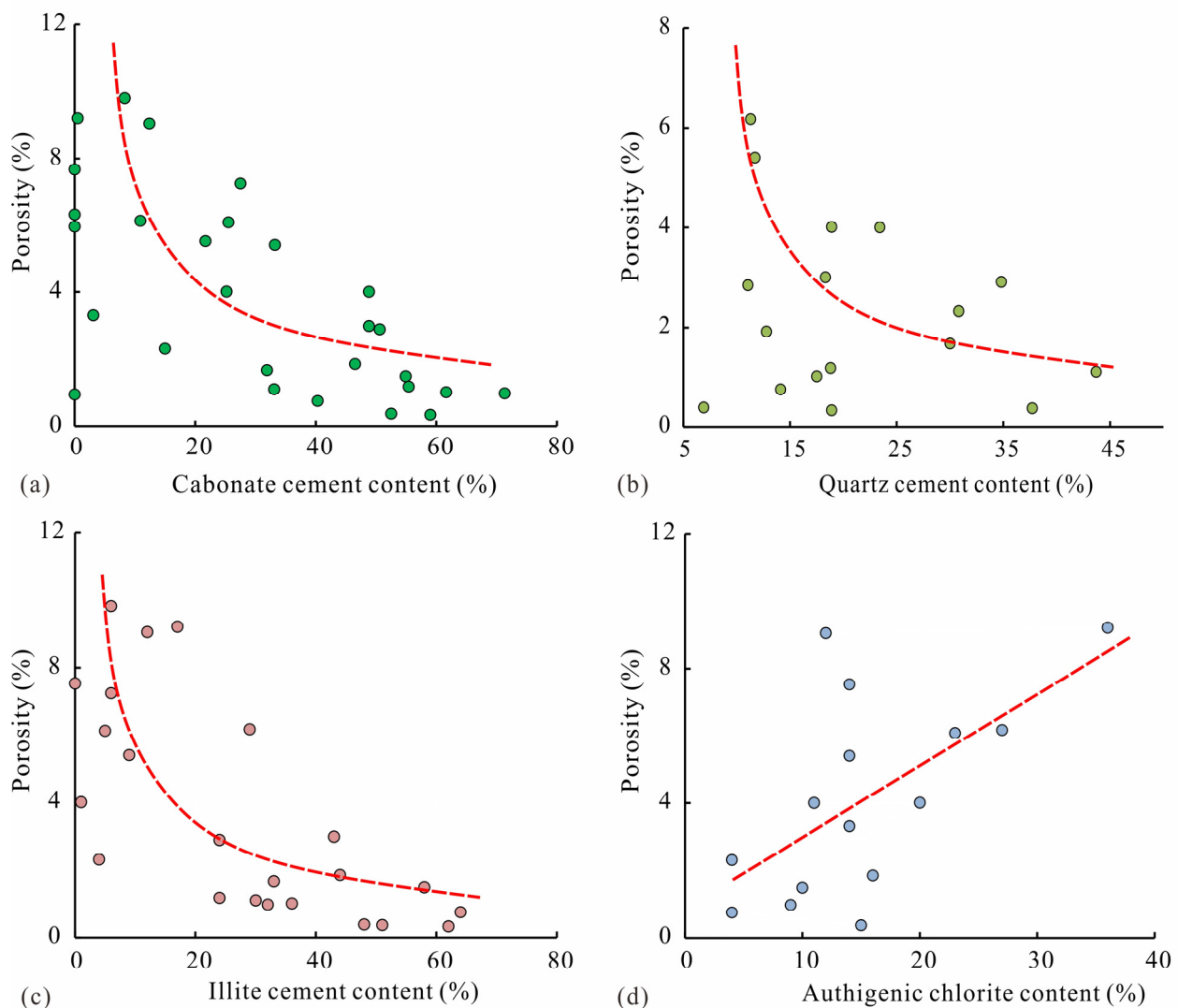


**Figure 11.** (a) Porosity and carbonate cement content. (b) Porosity and quartz cement content. (c) Porosity and illite content. (d) Porosity and authigenic chlorite content.

The phenomenon of quartz overgrowths can be observed in the rock samples, indicating that siliceous cementation is also an important diagenetic process in the tight oil reservoirs in the Lucaogou Formation. The transformation of clay minerals and the dissolution of feldspar grains provide a source of  $\text{SiO}_2$  for quartz precipitation; thus, siliceous cement usually occurs in the section of sandstone reservoirs that is rich in quartz grains [57]. The silica gel junction easily reduces the primary porosity of the reservoir, and quartz overgrowths can also reduce the width of the throat between clastic grains. The presence of quartz cement often leads to obvious bulges, and bulges between the clastic grains. Siliceous cement blocks the transport channel of the pore fluid so that the pores of the reservoir are reduced and the physical properties of the reservoir become worse (Figure 11b). Quartz cement has an influence on reservoir quality and belongs to the process of destructive diagenesis.

The presence of authigenic clay minerals has a destructive effect on diagenesis. Illite and I/S are fibrous, flaky, and honeycomb-like under SEM. These two minerals usually block the pore throat, affecting the quality of the reservoir (Figure 11c). Authigenic chlorite can protect the reservoir's primary pores to a certain extent, as chlorite rims can increase the reservoir's ability to resist compaction. On the other hand, reducing the width of the throat channel has a certain protective effect on the primary pores, and the cement content

of chlorite has a clear positive correlation with the porosity of the reservoir. It is shown that authigenic chlorite cementation can effectively protect the primary intergranular pores of tight oil reservoirs (Figure 11d).

Therefore, the filling phase of clay minerals related to illite is usually regarded as the damage factor of tight reservoirs. On the contrary, the clay mineral-filling phase related to authigenic chlorite usually has a relatively high porosity, which is the result of the retention of authigenic porosity and resistance to mechanical compaction [52]. Therefore, the relationship between the clay mineral cementation phase and reservoir properties cannot be clearly proved.

The Lucaogou Formation underwent the alternating dissolution of acid-base fluids [58], and feldspar grains and tuff components were dissolved to varying degrees. Chemically unstable feldspar grains in rock skeletons are susceptible to dissolution by acidic fluids (mainly atmospheric precipitation and organic acids) [30,59], and alkali tuff components may improve the quality of the reservoir through secondary pore formation by dissolution. The dissolution of feldspar grains can significantly improve the porosity of the reservoir during its formation, and secondary pores formed due to the dissolution effect are basically not affected by mechanical compacting in the later stage. The existence of secondary pores greatly improves the porosity of the reservoir. Thus, dissolution has a contributing effect on the improvement of reservoir quality (Figure 12). The dissolution facies of unstable components belongs to the process of constructive diagenesis, which can promote the improvement of reservoir quality.

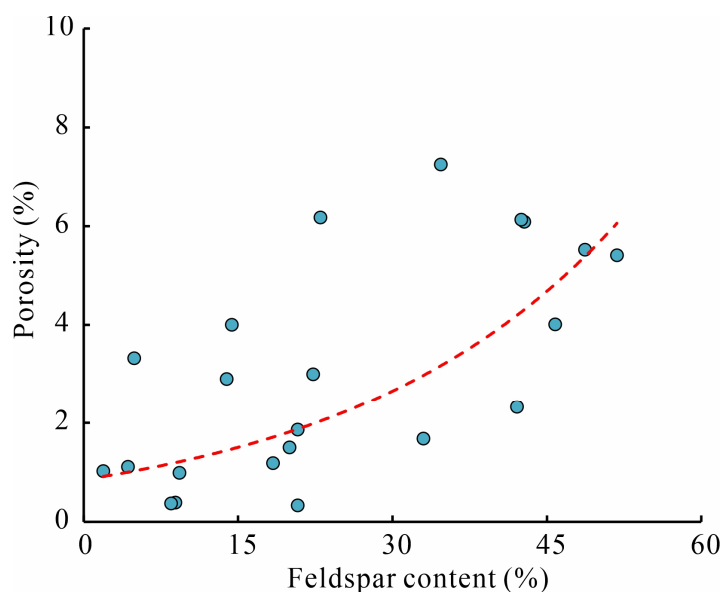


**Figure 12.** Diagram of the relationship between feldspar content and porosity.

### 5.3. Prediction of Diagenetic Facies and Favorable Reservoirs

The diagenetic facies of Well J174 in the tight oil reservoirs of the Lucaogou Formation was predicted by the established logging identification of the convolution neural network model. The type of single-well diagenetic facies in the study area was finally determined, and the vertical distribution law of single-well diagenetic facies was predicted according to the high vertical resolution of the logging curves.

The vertical distribution of the diagenetic facies in a single well shows that the study area mainly develops dissolution facies, carbonate cementation facies, and dissolution facies, whereas quartz cementation facies and clay mineral-filling facies are less developed. Comparing the predicted diagenetic facies types with the corresponding depth of thin sections and SEM images, the predicted results have a high coincidence rate, which indicates that the model has a certain guiding significance for the accurate identification of diagenetic

facies in tight oil reservoirs (Figure 13). From the conclusion of comprehensive logging interpretation, it can be seen that the dissolution facies develop in the interval whose mineral composition is mainly quartz and feldspar, as well as the interval with nuclear magnetic resonance (NMR) porosity and measured porosity, which has a high oil saturation value and is a favorable interval for reservoir development. Minerals are mainly composed of carbonate rocks because the cementation of carbonate rocks has a great influence on reservoir porosity; thus, the NMR porosity and the measured porosity of the reservoirs are both small and the oil saturation value is relatively low. Therefore, the reservoir physical properties corresponding to carbonate cementation facies-developed layers are the worst. Because of compaction, the NMR porosity is smaller than the measured porosity, and the oil content is poor. The physical properties of the reservoirs corresponding to the interval where quartz cementation facies and clay mineral-filling facies are developed are poor.

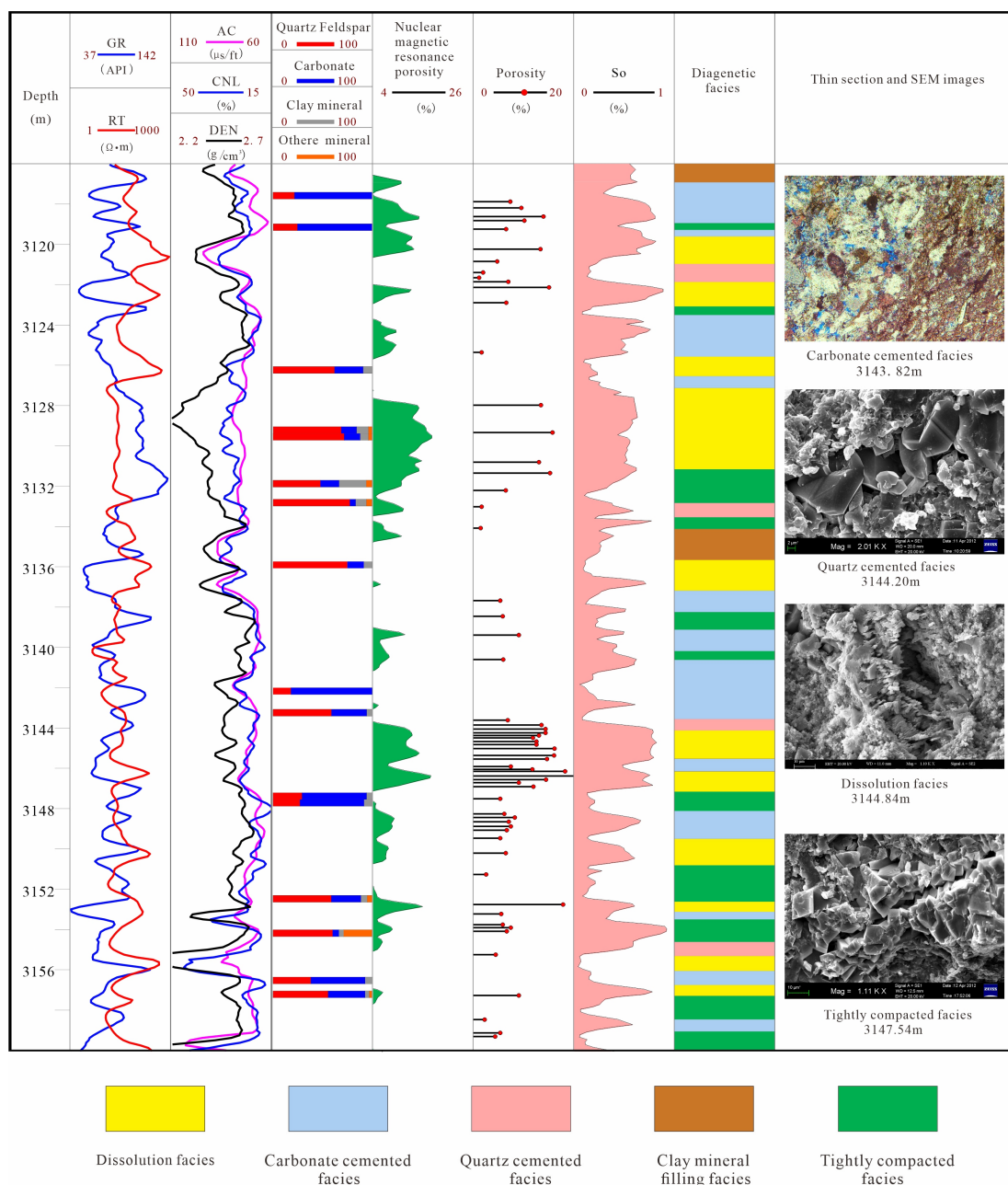


Figure 13. Well J174—single-well diagenetic facies prediction columnar diagram.

## 6. Conclusions

(1) Based on core analysis data, casting thin section observations, SEM analysis, and other data from the study area, diagenetic facies were divided and named according to the principle of mineral and diagenesis type, and can be classified into five diagenetic facies: tightly compacted facies, carbonate-cemented facies, clay mineral-filling facies, quartz-cemented facies, and dissolution facies.

(2) The selected GR, AC, DEN, RT, and CNL were sensitive to diagenetic facies, and were used to summarize the logging response characteristics of different types of diagenetic facies and to establish a diagenetic facies logging database. The convolution neural network model was introduced to build a logging identification model of diagenetic facies in the study area.

(3) On the basis of constructing the convolution neural network diagenetic facies model, taking Well J174 as an example, the diagenetic facies of this well were identified and divided, and the accuracy of the diagenetic facies prediction model was evaluated. The prediction results of the diagenetic facies were in good agreement with the microscopic observation results, and different types of diagenetic facies can be developed in different intervals. Combined with the relevant physical property analysis data, it shows that the intervals with poor reservoir physical properties and poor oil content in the study area were related to carbonate cementation facies, compacted tight diagenesis facies, quartz cementation facies and clay mineral-filling facies. The dissolution of unstable components corresponded to the main high-quality reservoirs and oil-bearing reservoirs of tight oil reservoirs in the study area, and the dominant diagenetic facies belt in the study area was also a favorable interval for finding the dominant reservoirs in the following stage.

**Author Contributions:** Conceptualization, M.Q.; funding acquisition, C.H.; methodology, C.H., C.M., G.L. (Geng Liu) and X.H.; software, G.L. (Geng Liu) and X.H.; supervision, C.H. and C.M.; validation, G.L. (Guan Li); writing—original draft, M.Q., Y.Y., R.S. and X.C.; writing—review and editing, M.Q., C.H., C.M., Y.Y., R.S. and X.C. All authors were informed about each step of the manuscript process, including submission, revision, revision reminder, etc., via emails from our system or the assigned Assistant Editor. All authors have read and agreed to the published version of the manuscript.

**Funding:** This work was jointly supported by the Natural Science Foundation of Xinjiang Uygur Autonomous Region (Grant No. 2020D01C037), the National Natural Science Foundation of China (Grant No. 42062010), the Opening Fund of Key Laboratory of Deep Oil and Gas (20CX02114A) and the Tianshan Innovation Team Program (2020D14023).

**Acknowledgments:** We are grateful to the anonymous reviewers for their insightful and constructive comments for improving the manuscript.

**Conflicts of Interest:** The authors declare no conflict of interest.

## References

1. Hu, S.-Y.; Zhu, R.-K.; Wu, S.-T.; Bai, B.; Yang, Z.; Cui, J.-W. Profitable exploration and development of continental tight oil in China. *Pet. Explor. Dev.* **2018**, *45*, 737–748. [[CrossRef](#)]
2. Milliken, K.L.; Curtis, M.E. Imaging pores in sedimentary rocks: Foundation of porosity prediction. *Mar. Pet. Geol.* **2016**, *73*, 590–608. [[CrossRef](#)]
3. Wang, M.; Lu, S.; Huang, W.; Liu, W. Pore characteristics of lacustrine mudstones from the Cretaceous Qingshankou Formation, Songliao Basin. *Interpretation* **2017**, *5*, T373–T386. [[CrossRef](#)]
4. Wang, J.-L.; Feng, L.-Y.; Steve, M.; Tang, X.; Gail, T.E.; Mikael, H. China's unconventional oil: A review of its resources and outlook for long-term production. *Energy* **2015**, *82*, 31–42. [[CrossRef](#)]
5. Zou, C.-N.; Zhang, G.-S.; Yang, Z.; Tao, S.-Z.; Hou, L.-H.; Zhu, R.-K.; Yuan, X.-J.; Ran, Q.-Q.; Li, D.-H.; Wang, Z.-P. Geological concepts, characteristics, resource potential and key techniques of unconventional hydrocarbon: On unconventional petroleum geology. *Pet. Explor. Dev.* **2013**, *40*, 385–399. [[CrossRef](#)]
6. Sonnenberg, S.A.; Pramudito, A. Petroleum geology of the giant Elm Coulee field, Williston Basin. *AAPG Bull.* **2009**, *93*, 1127–1153. [[CrossRef](#)]

7. Sun, L.; Tuo, J.; Zhang, M.; Wu, C.; Chai, S. Pore structures and fractal characteristics of nano-pores in shale of Lucaogou formation from Junggar Basin during water pressure-controlled artificial pyrolysis. *J. Anal. Appl. Pyrolysis* **2019**, *140*, 404–412. [[CrossRef](#)]
8. Clarkson, C.R.; Wood, J.M.; Burgis, S.E.; Aquino, S.D.; Freeman, M. Nanopore-Structure Analysis and Permeability Predictions for a Tight Gas Siltstone Reservoir by Use of Low-Pressure Adsorption and Mercury-Intrusion Techniques. *SPE Reserv. Eval. Eng.* **2012**, *15*, 648–661. [[CrossRef](#)]
9. Pollastro, R.-H. Total petroleum system assessment of undiscovered resources in the giant Barnett Shale continuous (unconventional) gas accumulation, Fort Worth Basin, Texas. *AAPG Bull.* **2007**, *91*, 551–578. [[CrossRef](#)]
10. Zha, M.; Wang, S.; Ding, X.; Feng, Q.; Xue, H.; Su, Y. Tight oil accumulation mechanisms of the Lucaogou Formation in the Jimsar Sag, NW China: Insights from pore network modeling and physical experiments. *J. Southeast Asian Earth Sci.* **2018**, *178*, 204–215. [[CrossRef](#)]
11. Yang, Y.; Qiu, L.; Wan, M.; Jia, X.; Cao, Y.; Lei, D.; Qu, C. Depositional model for a salinized lacustrine basin: The Permian Lucaogou Formation, Jimsar Sag, Junggar Basin, NW China. *J. Southeast Asian Earth Sci.* **2018**, *178*, 81–95. [[CrossRef](#)]
12. Du, J.-H.; Hu, S.-Y.; Pang, Z.-L.; Lin, S.-H.; Hou, L.-H.; Zhu, R.-K. The types, potentials and prospects of continental shale oil in China. *China Pet. Explor.* **2019**, *24*, 560–568.
13. Pang, H.; Pang, X.-Q.; Dong, L.; Zhao, X. Factors impacting on oil retention in lacustrine shale: Permian Lucaogou Formation in Jimusar Depression, Junggar Basin. *J. Pet. Sci. Eng.* **2018**, *163*, 79–90. [[CrossRef](#)]
14. Su, Y.; Zha, M.; Ding, X.; Qu, J.; Gao, C.; Jin, J.; Iglauer, S. Petrographic, palynologic and geochemical characteristics of source rocks of the Permian Lucaogou formation in Jimsar Sag, Junggar Basin, NW China: Origin of organic matter input and depositional environments. *J. Pet. Sci. Eng.* **2019**, *183*, 106364. [[CrossRef](#)]
15. Lin, M.; Xi, K.; Cao, Y.; Liu, Q.; Zhang, Z.; Li, K. Petrographic features and diagenetic alteration in the shale strata of the Permian Lucaogou Formation, Jimusar sag, Junggar Basin. *J. Pet. Sci. Eng.* **2021**, *203*, 108684. [[CrossRef](#)]
16. Pan, Y.; Huang, Z.; Guo, X.; Li, T.; Zhao, J.; Li, Z.; Qu, T.; Wang, B.; Fan, T.; Xu, X. Lithofacies types, reservoir characteristics, and hydrocarbon potential of the lacustrine organic-rich fine-grained rocks affected by tephra of the permian Lucaogou formation, Santanghu basin, western China. *J. Pet. Sci. Eng.* **2021**, *208*, 109631. [[CrossRef](#)]
17. Cao, Y.-C.; Zhu, N.; Zhang, S.-M.; Xi, K.-L.; Xue, X.-J. Diagenesis and Reserving Space Characteristics of Tight Oil Reservoirs of Permian Lucaogou Formation in Jimusar Sag of Junggar Basin, China. *J. Earth Sci. Environ.* **2019**, *41*, 253–266.
18. Cui, Y.-F.; Wang, G.-W.; Jones, S.J.; Zhou, Z.; Ran, Y.; Lai, J.; Li, R.; Deng, L. Prediction of diagenetic facies using well logs—A case study from the upper Triassic Yanchang Formation, Ordos Basin, China. *Mar. Pet. Geol.* **2017**, *81*, 50–65. [[CrossRef](#)]
19. Bjørlykke, K. Relationships between depositional environments, burial history and rock properties. Some principal aspects of diagenetic process in sedimentary basins. *Sediment. Geol.* **2014**, *301*, 1–14. [[CrossRef](#)]
20. Ran, Z.; Wang, G.-W.; Lai, J.; Zhou, Z.-L.; Cui, Y.-F.; Dai, Q.-Q.; Chen, J.; Wang, S.-C. Quantitative Characterization of Dia-genetic Facies of Tight Sandstone Oil Reservoir by Using Logging Crossplot: A case study on Chang 7 tight sandstone oil res-ervoir in Huachi area, Ordos Basin. *Acta Sedimentol. Sin.* **2016**, *34*, 694–706.
21. Karim, A.; Pe-Piper, G.; Piper, D. Controls on diagenesis of Lower Cretaceous reservoir sandstones in the western Sable Sub-basin, offshore Nova Scotia. *Sediment. Geol.* **2009**, *224*, 65–83. [[CrossRef](#)]
22. Munawar, M.-J.; Lin, C.-Y.; Cnudde, V.; Bultreys, T.; Dong, C.-M.; Zhang, X.-G.; De, B.-W.; Zahid, M.-A.; Wu, Y.-Q. Petro-graphic characterization to build an accurate rock model using micro-CT: Case study on low-permeable to tight turbidite sandstone from Eocene Shahejie Formation. *Micron* **2017**, *109*, 22–33. [[CrossRef](#)] [[PubMed](#)]
23. Okunuwadje, S.E.; Bowden, S.A.; Macdonald, D.I. Diagenesis and reservoir quality in high-resolution sandstone sequences: An example from the Middle Jurassic Ravenscar sandstones, Yorkshire Coast UK. *Mar. Pet. Geol.* **2020**, *118*, 104426. [[CrossRef](#)]
24. Lai, J.; Fan, X.-C.; Pang, X.-J.; Zhang, X.-S.; Xiao, C.-W.; Zhao, X.-J.; Han, C.; Wang, G.-W.; Qin, Z.-Q. Correlating diagenetic facies with well logs (conventional and image) in sandstones: The Eocene Suweiyi Formation in Dina 2 Gasfield, Kuqa de-pression of China. *J. Pet. Sci. Eng.* **2018**, *174*, 617–636. [[CrossRef](#)]
25. Wang, J.; Cao, Y.; Liu, K.; Liu, J.; Kashif, M. Identification of sedimentary-diagenetic facies and reservoir porosity and permeability prediction: An example from the Eocene beach-bar sandstone in the Dongying Depression, China. *Mar. Pet. Geol.* **2017**, *82*, 69–84. [[CrossRef](#)]
26. Li, Y.; Chang, X.; Yin, W.; Sun, T.; Song, T. Quantitative impact of diagenesis on reservoir quality of the Triassic Chang 6 tight oil sandstones, Zhenjing area, Ordos Basin, China. *Mar. Pet. Geol.* **2017**, *86*, 1014–1028. [[CrossRef](#)]
27. Shi, Y.-J.; Xiao, L.; Mao, Z.-Q.; Guo, H.-P. An identification method for diagenetic facies with well logs and its geological sig-nificance in low-permeability sandstones:A case study on Chang 8 reservoirs in the Jiyuan region, Ordos Basin. *Acta Pet. Sin.* **2011**, *32*, 820–828.
28. Zhang, X.-X.; Zou, C.-N.; Tao, S.-Z.; Xu, C.-C.; Song, J.-R.; Li, G.-H. Diagenetic Facies Types and Semiquantitative Evaluation of Low Porosity and Permeability Sandstones of the Fourth Member Xujiahe Formation Guangan Area, Sichuan Basin. *Acta Sedimentol. Sin.* **2010**, *28*, 50–57.
29. Lai, J.; Wang, G.-W.; Wang, S.-N.; Xin, Y.; Wu, Q.-K.; Zheng, Y.-Q.; Li, J.-D.; Cang, D. Overview and research progress in logging recognition method of clastic reservoir diagenetic facies. *J. Cent. South Univ. (Sci. Technol.)* **2013**, *44*, 4942–4953.
30. Lai, J.; Wang, G.; Wang, S.; Cao, J.; Li, M.; Pang, X.; Zhou, Z.; Fan, X.; Dai, Q.; Yang, L.; et al. Review of diagenetic facies in tight sandstones: Diagenesis, diagenetic minerals, and prediction via well logs. *Earth-Sci. Rev.* **2018**, *185*, 234–258. [[CrossRef](#)]

31. Ozkan, A.; Cumella, S.P.; Milliken, K.L.; Laubach, S.E. Prediction of lithofacies and reservoir quality using well logs, Late Cretaceous Williams Fork Formation, Mamm Creek field, Piceance Basin, Colorado. *AAPG Bull.* **2011**, *95*, 1699–1723. [[CrossRef](#)]
32. Wang, C.-W.; Ma, D.-X.; Tian, B.; Liang, J.-S.; Wang, Q.; Liu, T.-S. Diagenetic Evolution and Facies of Shanxi Formation in LX Area of Ordos Basin. *Acta Sedimentol. Sin.* **2016**, *34*, 594–605.
33. Zhu, P.; Lin, C.-Y.; Wu, P.; Fan, R.-F.; Wang, D.-R.; Liu, X.-L. Logging quantitative identification of diagenetic facies by using principal component analysis: A case of Es3x1 in Zhuang 62-66 Area, Wu Hao-zhuang Oil field. *Prog. Geophys.* **2015**, *30*, 2360–2365.
34. Hinton, G.E.; Osindero, S.; Teh, Y.W. A fast learning algorithm for deep belief nets. *Neural Comput.* **2006**, *18*, 1527–1554. [[CrossRef](#)]
35. Sungil, K.; Kyungbook, L.; Minhui, L.; Taewoong, A.; Jaehyoung, L.; Hwasoo, S.; Ning, F.-L. Saturation Modeling of Gas Hydrate Using Machine Learning with X-Ray CT Images. *Energies* **2020**, *13*, 5032.
36. Wang, P.; Cao, Y.; Shen, C.; Liu, L.; Shen, H.T. Temporal Pyramid Pooling-Based Convolutional Neural Network for Action Recognition. *IEEE Trans. Circuits Syst. Video Technol.* **2016**, *27*, 2613–2622. [[CrossRef](#)]
37. Shan, L.-Q.; Liu, Y.-C.; Tang, M.; Yang, M.; Bai, X.-Y. NN-BiLSTM hybrid neural networks with attention mechanism for well log prediction. *J. Pet. Sci. Eng.* **2021**, *205*, 108838. [[CrossRef](#)]
38. Wu, H.; Li, Z.; Liu, N.; Zhang, B. Improved seismic well tie by integrating variable-size window resampling with well-tie net. *J. Pet. Sci. Eng.* **2021**, *208*, 109368. [[CrossRef](#)]
39. Zhang, Y.; Zhang, C.; Ma, Q.; Zhang, X.; Zhou, H. Automatic prediction of shear wave velocity using convolutional neural networks for different reservoirs in Ordos Basin. *J. Pet. Sci. Eng.* **2021**, *208*, 109252. [[CrossRef](#)]
40. Zhang, Z.-H.; Tian, J.-J.; Han, C.-C.; Zhang, W.-W.; Deng, S.-W.; Sun, G.-X. Reservoir characteristics and main controlling factors of Lucaogou Formation in Jimsar Sag, Junggar Basin. *Lithol. Reserv.* **2021**, *33*, 116–126.
41. Shao, Y.; Yang, Y.-Q.; Wan, M.; Qiu, W.-L.; Cao, Y.-C.; Yang, S.-C. Sedimentary Characteristic and Facies Evolution of Permian Lucaogou Formation in Jimsar Sag, Junggar Basin. *Xinjiang Pet. Geol.* **2015**, *36*, 635–641.
42. Qiu, Z.; Zou, C.; Dong, D.; Lu, B.; Shi, Z.; Tao, H.; Zhou, J.; Lei, D.; Zhang, C. Petroleum system assessment of conventional-unconventional oil in the Jimusar sag, Junggar basin, Northwest China. *J. Unconv. Oil Gas Resour.* **2016**, *16*, 53–61. [[CrossRef](#)]
43. Ma, K.; Hou, J.-G.; Liu, Y.-M.; Shi, Y.-Q.; Yan, L.; Chen, F.-L. The sedimentary model of saline lacustrine mixed sedimentation in Permian Lucaogou Formation, Jimsar sag. *Acta Pet. Sin.* **2017**, *38*, 636–648.
44. Wang, Y.; Teng, Q.; He, X.; Feng, J.; Zhang, T. CT-image of rock samples super resolution using 3D convolutional neural network. *Comput. Geosci.* **2019**, *133*, 104314. [[CrossRef](#)]
45. Lima, R.-P.-D.; Duarte, D.; Nicholson, C.; Slatt, R.; Marfurt, K.-J. Petrographic microfacies classification with deep convolutional neural networks. *Comput. Geosci.* **2020**, *142*, 104481. [[CrossRef](#)]
46. Cunha, A.; Pochet, A.; Lopes, H.; Gattass, M. Seismic fault detection in real data using transfer learning from a convolutional neural network pre-trained with synthetic seismic data. *Comput. Geosci.* **2019**, *135*, 104344. [[CrossRef](#)]
47. Zha, M.; Su, Y.; Gao, C.-H.; Qu, J.-X.; Wang, X.-L.; Ding, J.-X. Tight reservoir space characteristics and controlling factors: An example from Permian Lucaogou formation in Jimsar sag, Junggar basin, northwest China. *J. China Univ. Min. Technol.* **2017**, *46*, 85–95.
48. Lai, J.; Wang, G.-W.; Wang, S.-N.; Zheng, Y.-Q.; Wu, H.; Zhang, Y.-C. Research Status and Advances in the Diagenetic Facies of Clastic Reservoirs. *Adv. Earth Sci.* **2013**, *28*, 39–50.
49. Li, P.; Liu, Z.-D.; Chen, Y.-M.; Zhao, J.-H. Summarization of application for identifying diagenetic facies in low porosity and low permeability reservoirs using well-logging information. *Prog. Geophys.* **2017**, *32*, 183–190.
50. Lai, J.; Wang, G.; Chai, Y.; Ran, Y. Prediction of Diagenetic Facies using Well Logs: Evidences from Upper Triassic Yanchang Formation Chang 8 Sandstones in Jiyuan Region, Ordos Basin, China. *Oil Gas Sci. Technol.—Rev. D’ifr Energ. Nouv.* **2015**, *71*, 34. [[CrossRef](#)]
51. Dutton, S.-P.; Loucks, R.-D. Diagenetic controls on evolution of porosity and permeability in lower Tertiary Wilcox sandstones from shallow to ultradeep (200–6700 m) burial, Gulf of Mexico Basin, U.S.A. *Mar. Pet. Geol.* **2010**, *27*, 69–81. [[CrossRef](#)]
52. Wu, D.; Liu, X.; Du, Y.; Jiang, L.; Cheng, Z. Predictive distribution of high-quality tight reservoirs of coarse clastic rocks by linking diagenesis to sedimentary facies: Evidence from the upper Sha 4 Member in the northern Bonan Sag, Bohai Bay Basin, eastern China. *Interpretation* **2018**, *6*, T413–T429. [[CrossRef](#)]
53. Higgs, K.; Crouch, E.; Raine, J. An interdisciplinary approach to reservoir characterisation; an example from the early to middle Eocene Kaimiro Formation, Taranaki Basin, New Zealand. *Mar. Pet. Geol.* **2017**, *86*, 111–139. [[CrossRef](#)]
54. Henares, S.; Caracciolo, L.; Cultrone, G.; Fernández, J.; Viseras, C. The role of diagenesis and depositional facies on pore system evolution in a Triassic outcrop analogue (SE Spain). *Mar. Pet. Geol.* **2014**, *51*, 136–151. [[CrossRef](#)]
55. Luo, L.; Meng, W.; Gluyas, J.; Tan, X.; Gao, X.; Feng, M.; Kong, X.; Shao, H. Diagenetic characteristics, evolution, controlling factors of diagenetic system and their impacts on reservoir quality in tight deltaic sandstones: Typical example from the Xujiahe Formation in Western Sichuan Foreland Basin, SW China. *Mar. Pet. Geol.* **2019**, *103*, 231–254. [[CrossRef](#)]
56. Houseknecht, D.W. Assessing the Relative Importance of Compaction Processes and Cementation to Reduction of Porosity in Sandstones. *AAPG Bull.* **1987**, *71*, 633–642. [[CrossRef](#)]
57. Worden, R.H.; Mayall, M.; Evans, I.J. The Effect of Ductile-Lithic Sand Grains and Quartz Cement on Porosity and Permeability in Oligocene and Lower Miocene Clastics, South China Sea: Prediction of Reservoir Quality. *AAPG Bull.* **2000**, *84*, 345–359.

- 
58. Wang, J.; Zhou, L.; Liu, J.; Zhang, X.; Zhang, F.; Zhang, B. Acid-base alternation diagenesis and its influence on shale reservoirs in the Permian Lucaogou Formation, Jimusar Sag, Junggar Basin, NW China. *Pet. Explor. Dev.* **2020**, *47*, 962–976. [[CrossRef](#)]
  59. Lai, J.; Wang, G.; Ran, Y.; Zhou, Z.; Cui, Y. Impact of diagenesis on the reservoir quality of tight oil sandstones: The case of Upper Triassic Yanchang Formation Chang 7 oil layers in Ordos Basin, China. *J. Pet. Sci. Eng.* **2016**, *145*, 54–65. [[CrossRef](#)]